Green Synthesis of CuO and Se Nanoparticles and CuO/Se Agglomerates of NPs by *Anabasis setifera* Biomass Extract: Antimicrobial, Antioxidant, Antibiofilm, and Anticancer Activities

Mohamed H. El-Sayed,^a Hussam M. Shubaily,^b Mostafa I. Abdelglil,^c Naifa Alenazi,^d Salama A. Salama,^e E. K. Abdel-Khalek,^f Mohamed H. Sharaf,^{g,*} and Mohamed A. Amin ^{g,*}

Anabasis setifera shoot extract was utilized in this study as a stabilizing agent to synthesize Se and CuO nanoparticles (NPs), as well as CuO/Se agglomerates of NPs in a biologically safe manner, and these nanoparticles were then employed as antibacterial, antioxidant, antibiofilm, and anticancer agents. Transmission electron microscopy confirmed the irregular, spherical, and agglomerate shapes of Cu, Se, and CuO/Se, respectively. The EDS mapping of the CuO/Se agglomerates of NPs showed that all elements were uniformly distributed. Among all examined treatments, the CuO/Se agglomerates of NPs showed the strongest antimicrobial action, with inhibition zones ranging from 19 mm for Klebsiella pneumoniae to 26.1 mm for Bacillus cereus, so further testing was done only with CuO/Se agglomerates of NPs. The findings demonstrated that the antioxidant activity of CuO/Se agglomerates of NPs was 150 ug/mL for the 2.2-diphenyl-1-picrylhydrazyl (DPPH) method. compared to 8.9 µg/mL for ascorbic acid, and 135 µg/mL for the 2,2'azinobis-(3-ethylbenzo-thiazoline-6-sulfonic acid (ABTS) method, compared to 7.61 µg/mL for ascorbic acid. Se/Cu repressed the proliferation of Mcf7 and HepG2 cells, but CuO/Se showed more activity against HepG2 cells with an IC50 of 322.5 µg/mL. CuO/Se agglomerates of NPs based on Anabasis setifera extract serve as a stabilizing agent, exhibiting a biological activity profile that makes them appealing choices for various biomedical applications.

DOI: 10.15376/biores.20.4.10008-10027

Keywords: Anabasis setifera; Selenium; Copper; Nanoparticles; Anticancer; Antimicrobial

Contact information a: Department of Biological Sciences, College of Science, Northern Border University, Arar, Saudi Arabia; b: Basic Medical Sciences Department, Faculty of Medicine, Jazan University, Jazan, Saudi Arabia; c: College of Pharmacy, Al-Farahidi University- Baghdad- Iraq; d: Department of Pharmaceutical Science, College of Pharmacy, Princess Nourah Bint Abdulrahman University, P.O. Box 84428, Riyadh 11671, Saudi Arabia; e: Department of Biology, College of Science, Jazan University, P.O. Box. 114, Jazan 45142, Kingdom of Saudi Arabia; f: Department of Physics, Faculty of Science, Al-Azhar University, Nasr City 11884, Cairo, Egypt; g: Botany and microbiology Department, Faculty of Science, Al-Azhar University Cairo 11884, Egypt;

^{*} Corresponding author: mamin7780@azhar.edu.eg; mohamed.sharaf@azhar.edu.eg

INTRODUCTION

The synthesis of metal nanoparticles using plant and fungal extracts has emerged as a sustainable alternative to conventional chemical methods, leveraging phytochemicals as stabilizing agents (Amin *et al.* 2024, 2025; Selim *et al.* 2025a, b). Copper nanoparticles (CuO NPs) and selenium nanoparticles (SeNPs) are particularly notable for their distinct biological and catalytic properties.

CuO NPs exhibit antimicrobial and catalytic activities due to their high surface-to-volume ratio and redox potential (Ryntathiang *et al.* 2024). While SeNPs demonstrate antioxidant, anticancer, and photoprotective capabilities, combining these metals into a hybrid consortium could synergistically enhance their functional properties, offering multifunctional nanomaterials for both biomedical and environmental applications (El-Batal *et al.* 2023; Soliman *et al.* 2024; Abd-ElGawad *et al.* 2025). Additionally, a study revealed that CuO NPs possess unique physicochemical properties, including fungicidal, antibacterial, medicinal, optical, and catalytic effects. The surface, biocompatibility, and physical and chemical properties of nanocomposite materials are improved by doping them with various metals (Al-Rajhi *et al.* 2022).

Green synthesis approaches using plant extracts, such as *Anabasis setifera*, capitalize on polyphenols, flavonoids, and alkaloids to reduce metal ions and stabilize nanoparticles. These phytochemicals not only mediate nanoparticle formation but also contribute to bioactivity, as seen in SeNPs' tyrosinase inhibition and CuO NPs' antibacterial effects by causing conformational changes and dimming the enzyme's intrinsic fluorescence.

Also, SeNPs bind to the enzyme *via* non-covalent forces such hydrogen bonds and van der Waals forces, thereby reducing tyrosinase activity. Reactive oxygen species (ROS) and Cu⁺ and Cu²⁺ ion release are the main ways that copper oxide nanoparticles (CuO NPs) cause bacterial cell damage and exhibit antibacterial properties. (Khowdiary *et al.* 2024).

In a previous study, the authors found that the *Anabasis setifera* shoot extract includes a number of important phenolic components, including coumaric acid, gallic acid, ferulic acid, chlorogenic acid, and rutin (Amin *et al.* 2024). Also, Abdelaziz *et al.* (2024) showed that ethyl acetate extract of *Anabasis setifera* is a rich source of important phytochemicals, with a total phenolic content of 4,264 µg/mL, which indicates significant biological and pharmacological potential. All of these active compounds confirm the high efficiency of this extract in reducing bulk material to the nano scale.

The proposed use of *Anabasis setifera* water extract aligns with eco-friendly synthesis trends, minimizing toxic byproducts. Future research should focus on optimizing reaction parameters (*e.g.*, temperature, pH). The current study is original in many important ways, including a novel green synthesis strategy for Se and CuO NPs, and CuO/Se agglomerates production by using a medicinal plant as a stabilizer and capping agent. According to the high efficiency of CuO/Se on multidrug-resistant bacteria, which is greater than that of CuO or Se individually, CuO/Se agglomerates represent a promising new avenue for creating multifunctional nanomaterials with improved therapeutic effectiveness through antibiofilm, anticancer, and antioxidant applications.

EXPERIMENTAL

Extraction of Plant Extract

The collected material of *Anabasis setifera* shoot (from Wadi Hoff- western desert- Egypt) was cleaned with distilled deionized water and allowed to dry at room temperature for five days in the shade. Five grams of the plant powder and 100 mL of double-distilled deionized water were then heated for 20 min at 70 °C. After being further filtered *via* Whatman No. 1 filter paper, this solution was stored at 4 °C.

Biogenic Synthesis of Se and CuO NPs, and CuO/Se Agglomerates

SeNPs were synthesized by mixing 100 mL of 10 mM Na₂SeO₃ with 20 mL of the extract. The reaction was magnetically agitated at 1200 rpm, at room temperature for an entire day. The reaction was conducted in a darkened environment with constant magnetic stirring. Se-NPs were gathered and dehydrated (Soliman *et al.* 2024).

To create CuO NPs, at room temperature, 50 mL of a 1 mM copper sulphate solution were progressively mixed with 25 mL of plant extract. CuO NPs were then created by heating the mixture for 4 h at 70 °C. Centrifugation was used to separate these NPs. Pure CuO NP was obtained after a final calcination phase that lasted 4 h at 500 °C (Gad *et al.* 2025)

Copper sulfate (1 mM) and sodium selenite (1 mM) were used to produce CuO/Se agglomerates. For 1 h at 40 °C, 30 mL of plant extract were continuously mixed using a magnetic stirrer. To remove any leftover plant organic residue, the Se, CuO, and CuO/Se were carefully washed three times in double-distilled deionized water after these NPs were collected by centrifuging it for 20 min at 10,000 rpm. Hot air was then used to dry it (Abd-ElGawad *et al.* 2025).

Characterisation of NPs

Cu K α radiation (λ = 1.5406 Å) with a range of 2θ from 20 to 80° at a scanning rate of 0.02° was used in a Bruker D8 Discover X-ray diffractometer to analyze the X-ray diffraction (XRD) patterns of the CuO, Se, and CuO/Se materials. Fourier transformation infrared (FTIR) spectra of *Anabasis setifera*, CuO, Se, and CuO/Se were taken by Thermo Scientific Nicolet iS50 FT-IR spectrometer in the range 4000 to 400 cm⁻¹. A JEM-2100 PLUS electron microscope (JEOL, Japan) operating at 200 kV with a LaB6 source was used to acquire transmission electron microscopy (TEM) pictures and selected area electron diffraction (SAED) patterns of CuO, Se, and CuO/Se materials. Using a JEM-2100 F (URP) apparatus set at 200 kV and fitted with a Dry SD30GV detector, the energy dispersive X-ray spectroscopy (EDS) analysis of these NPs and the EDS elemental mapping analysis of the CuO/Se solids were ascertained.

Selection of Isolates

The bacteriology laboratory of the Botany and Microbiology Department at Al-Azhar University provided the bacterial isolates used in this investigation as test microorganisms. Gram-negative bacteria, such as *Klebsiella pneumonia* and *Escherichia coli*, were among these microbes, as well as the Gram-positive species *Bacillus cereus* and *Staphylococcus aureus* (MRSA). The identification and antibiotic susceptibility testing were conducted previously using the VITEK2 system (BioMérieux, Inc., Durham, NC, USA) (Sharaf *et al.* 2021; El-Didamony *et al.* 2024). In addition to these bacterial strains,

Candida albicans was employed for testing the antimicrobial activity and biofilm inhibition due to the CuO/Se.

Antimicrobial Activity

On Muller Hinton agar (MHA, India) for bacteria and potato dextrose agar (PDA) for *Candida albicans*, the antimicrobial properties of extract from *Anabasis setifera*, selenium nanoparticles, copper nanoparticles, and bimetallic biogenesis CuO/Se agglomerates were assessed. *Staphylococcus aureus* (MRSA), *B. cereus*, *C. albicans*, *K. pneumoniae*, and *E. coli* isolates were cultivated for 24 h on the surface of prepared MHA and PDA for bacteria and fungi, respectively. A sterile cork borer was used to cut wells (6 mm), into which 100 µL of each compound was inserted. The wells were then left at 4 °C for 2 h. The plates were incubated for 24 h at 37 °C for the bacteria and 48 h at 28 °C for the *Candida albicans*. Ceftazidime 30 µg was used as a control for the bacterial strain, and Clotrimazole 10 µg was used as a control for the *Candida albicans*. After incubation, the inhibition zones were measured and recorded (Hsueh *et al.* 2010; Sharaf *et al.* 2021).

Determination of Minimum Inhibitory Concentration (MIC)

The MIC levels were determined for *E. coli*, *K. pneumonia*, *B. cereus*, and *S. aureus* (MRSA) using CuO/Se agglomerates, which were chosen for their strong effectiveness against bacteria and *Candida albicans*, as determined by the broth microdilution technique (El-Didamony *et al.* 2024). After three iterations of the experiment in duplicate, mean values were determined (El-Sherbiny *et al.* 2022).

Antioxidant Activity

DPPH assay

CuO/Se NPs' antioxidant activity was assessed using the DPPH (2, 2-diphenyl-1-picrylhydrazyl) technique, which was modified slightly by El-Sayed *et al.* (2022). The DPPH radical cation technique was adjusted to assess CuO/Se agglomerates' capacity to scavenge free radicals. For the DPPH reagent, 8 mg of DPPH was dissolved in 100 mL of MeOH, resulting in a solution concentration of 80 μ L/mL. A total of 100 μ L of DPPH reagent and 100 μ L of different concentrations of NPs (1000, 500, 250, 125, 62.5, 31.25, 15.62, and 7.81 μ g/mL) were combined in a 96-well microplate, and the mixture was incubated for 30 min at room temperature to ascertain the scavenging activity. An ELISA reader (TECAN, Groding, Austria) was used to measure the absorbance at 490 nm following incubation, with 100% methanol serving as a control. To calculate the DPPH scavenging effect, the following formula was used:

DPPH scavenging activity (%) =
$$\frac{\text{control absorbance} - \text{Cu-Se NPs absorbance}}{\text{control absorbance}} X100$$
 (1)

The effective dose of CuO/Se agglomerates required to scavenge DPPH radicals (at a 50% level) was measured and reported as the IC50 quantity.

ABTS Assay

ABTS is another assay used to assess antioxidant activity (2,2'-azino-bis(3-ethylbenzothiazoline-6-sulfonic acid)). With some slight adjustments, the ABTS assay was utilized to assess the antioxidant activity of CuO/Se agglomerates in accordance with Lee's (2015) methodology.

ABTS scavenging activity =
$$\frac{\text{control absorbance} - (\text{CuO-Se NPs}) \text{ absorbance}}{\text{control absorbance}} X100$$
 (2)

In Vitro Anti-Biofilm Ability

To assess the anti-biofilm capabilities, 96-well microtiter (flat-bottom, polystyrene) plates were used, utilizing a modified version of the Sharaf (2020) method. The procedure involved filling each well of sterile microtiter plates with 100 μ L of MHB and then inoculating them with 10 μ L of an overnight bacterial and *Candida* yeast culture solution (OD620 0.05 \pm 0.02). The mixture was mixed with 100 μ L of CuO/Se agglomerates at concentrations of 1/2 × MIC, 1/4 × MIC, and 1/8 × MIC. The plates were then incubated at 37 °C for 48 h. Following a 30-min incubation period, the biofilms were fixed with 100% ethanol and stained with crystal violet (0.1%, w/v). Following drying, 200 mL of 33% acetic acid was added, and a microplate reader set to 630 nm was used to measure the optical densities (OD) of the adhering organisms that had been stained. The following Eq. 3 was used to determine the percentage of inhibition of biofilm formation:

Biofilm inhibition (%) = 1 -
$$\frac{\text{OD630 of cells treated with different concentration of Cu-Se BNPs}}{\text{OD630 of non treated control}} \times 100$$
 (3)

Cell Culture and MTT Assay

Breast cancer (Mcf7) and hepatocellular carcinoma (HepG2) cell lines were used to test the cytotoxicity of plant-synthesized bi-metallic CuO/Se agglomerates using the MTT test technique. Cells in the logarithmic growth phase were used for the investigations. Cells were cultivated overnight in complete growth media after being seeded into each well of 96-well plates with a flat bottom. The medium was then removed and replaced with 0.1 mL of fresh DMEM containing either cisplatin or topotecan (IC50 55.74 \pm 0.72 $\mu g/mL$ of Mcf7 and 49.02 \pm 0.56 $\mu g/mL$ of HepG2) in the substance being tested. The plates were incubated at 37 °C for 72 h. After treatment, the plates were incubated for another 3 h at 37 °C after each well was treated with 20 μ L of the labeling indicator for MTT (CellTiter 96 AQueous One Solution Cell Proliferation Assay, Promega, Madison, WI, USA). The spectrophotometric absorbance of the samples at 480 nm with a reference wavelength of 630 nm following MTT incubation was measured using a Vario Scan Flash microplate reader (Thermo Fisher Scientific, Waltham, MA, USA) (Van de Loosdrecht *et al.* 1994).

Statistical Analysis

For statistical computations at the 0.05 level of probability, the authors utilized Minitab 18 (Stat Ease Inc., State College, PA, USA). Analyses of variance, *post hoc* Tukey's test, and one-way ANOVA were employed to examine quantitative data with a parametric distribution.

RESULTS and DISCUSSION

Crystal Structure and Microstructure Analysis of Se, CuO, and CuO/Se

Figure 1 displays the XRD patterns for the CuO, Se, and CuO/Se. The XRD pattern for CuO showed the formation of monoclinic structure of CuO nanoparticles, which

matched with JCPDS card No. 80-1268 (Sahooli *et al.* 2012; Vinu *et al.* 2021). Additionally, there are other impurity peaks (stars in Fig. 1) that may be due to the presence of phytochemicals of the plant extract. The XRD pattern for Se showed the formation of trigonal structure of Se nanoparticles that matched with JCPDS card No. 006-0362 (Vinu *et al.* 2021). The XRD pattern for CuO/Se showed the formation of monoclinic structure of CuO nanoparticles and trigonal structure of Se nanoparticles, which matched with JCPDS card No. 80-1268 and JCPDS card No. 006-0362, respectively (Sahooli *et al.* 2012; Vinu *et al.* 2021). From this observation, the combination of CuO and Se nanoparticles leads to the lower intensities, which may be attributed to the obstructive influence of the amorphous particles (Elkady *et al.* 2025).

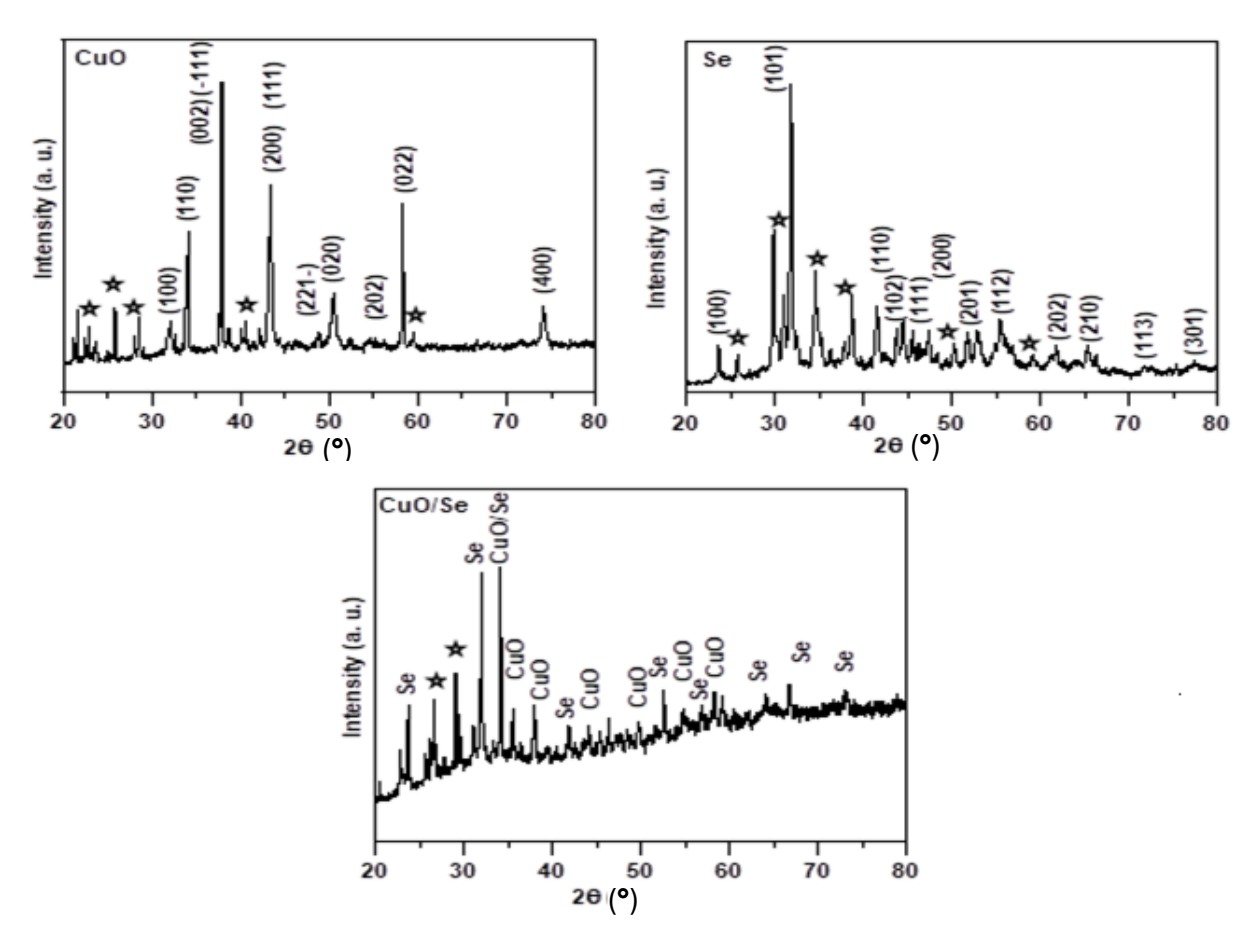


Fig. 1. XRD of CuO, Se, and CuO/Se, respectively

Figure 2 shows the FTIR transmittance spectra for the *Anabasis setifera* shoot, CuO, Se, and CuO/Se. The FTIR spectrum of *A. setifera* shoot revealed the presence of bands at 3419, 2925, 1635, 1370, and 1035 cm⁻¹. These features indicated functional groups of *A. setifera* shoot, in agreement with a report for *A. setifera* by Nowrouzi *et al.* (2025). The band at 3363 cm⁻¹ is attributed to the stretching vibration of many hydroxyls in the oligosaccharide of saponin chain. The bands at 2925 and 1635 cm⁻¹ are due to the C–H aliphatic sapogenin saponin graft and C–C bond in sapogenin, respectively. The bands at 1370 and 1035 cm⁻¹ are due to the O–H bond and the C–O stretching vibration. The FTIR spectrum of CuO NPs revealed the presence of extra bands at 515 and 619 cm⁻¹ with

functional groups of A. setifera shoot. The extra bands are due to the vibration band of Cu-O, which indicates the presence of CuO nanoparticles (Asaad et al. 2025). The FTIR spectrum of Se NPs revealed the presence of extra bands at 404, 445, and 829 cm⁻¹ with functional groups of A. setifera shoot. The extra bands at 404, 445 and 632 cm⁻¹ are due to the vibration band of Se-O while the band at 829 cm⁻¹ is due to the Se nanoparticles (Asaad et al. 2025). The FTIR spectrum of CuO/Se revealed extra bands at 404, 443, 543, and 603 cm⁻¹ with functional groups of A. setifera shoot. The extra bands at 404, 443 cm⁻¹ at are attributed to the vibration band of Se-O, while the bands at 543, and 603 cm⁻¹ are due to the vibration of Cu-O (Duman et al. 2016 and Muthu and Sridharan 2018). The presence of bands at 443 and 543 cm⁻¹ indicates the formation of CuO/Se material (Elkady et al. 2025). The appearance of new bands at 889 and 935 cm⁻¹ may be due to stretching vibrations of C-O and C-C, while the bands at 987 and 1240 cm⁻¹ may be due to bending C-O-H, and C-O-C vibrations (Tugarova et al 2018). The presence of these bands indicated that the biomacromolecules are capping the CuO/Se surface, in agreement with the following TEM results (Tugarova et al. 2018). Moreover, the appearance of new bands at 2141 and 2262 cm⁻¹ may be because of the formation of metal-oxygen bonds (Elkady et al. 2025).

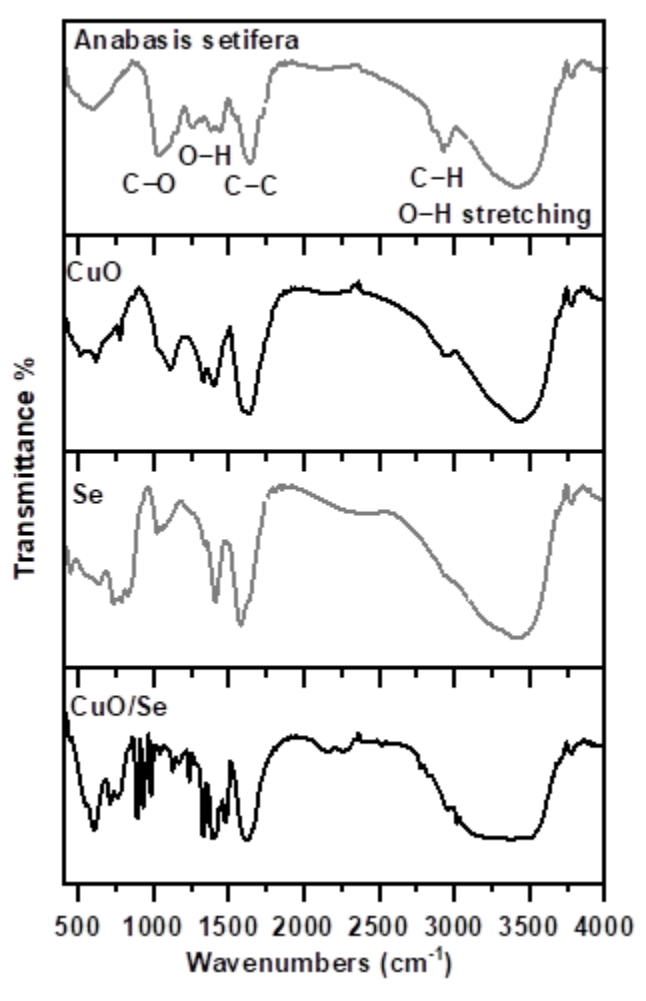


Fig. 2. The FTIR transmittance spectra for the Anabasis setifera, CuO, Se, and CuO/Se

Figure 3 (a) displays TEM images, (b) the histograms of the particle size distribution, and (c) SAED patterns of CuO, Se, and CuO/Se, respectively. The TEM image of the Cu NPs showed non-aggregated irregular and spherical shapes, while the TEM image of the Se NPs showed homogeneous (regular morphology) and non-aggregated spherical shapes (Hong *et al.* 2002; Thirupathi *et al.* 2024; Asaad *et al.* 2025). Further, the TEM image of CuO/Se displays spherical shapes of CuO/Se particles, spherical agglomerated morphology of Se nanoparticles, and irregular shapes of CuO particles (Rong *et al.* 2012). The histogram of the particle size distribution of the Se NPs showed a narrow size distribution, indicating the uniform distribution of the particle size. According to these histograms, the estimated average particle size of CuO, Se, and CuO/Se from histograms were found to be 80.97±20.42, 26.20±4.21, and 143.56±20.55 nm, respectively. These values indicate that the CuO and Se NPs were in the nanometer size range while the CuO/Se NP aggregates were larger than 100 nm.

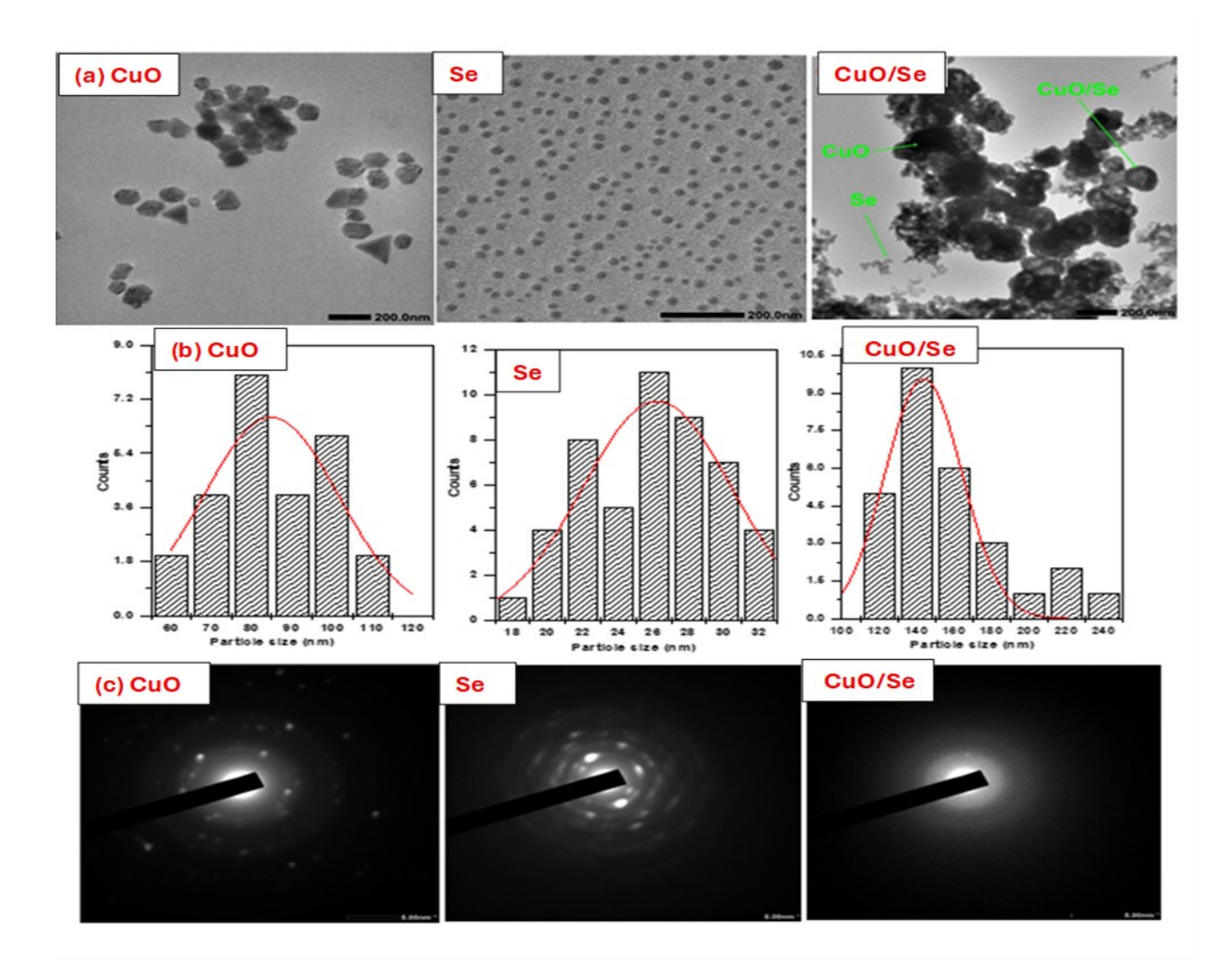


Fig. 3. TEM images (a), size distribution (b), and SAED patterns (c) of CuO, Se, and CuO/Se

From this result, the average particle size of CuO/Se was higher than that of CuO and Se NPs, which can be attributed to the integration of the outer Se with the inner CuO

(Asaad *et al.* 2025). Figure 3 also displays the SAED patterns of CuO, Se, and CuO/Se. The SAED patterns of these NPs display concentric rings with diffraction spots, which indicate the presence of polycrystalline nature of these NPs (Elkady *et al.* 2025). Figure 4 shows the EDS spectra of the CuO, Se, and CuO/Se. The EDS spectrum of the CuO NPS shows the presence of Cu, C, and O elements, while the EDS spectrum of the Se NPs shows the presence of Se element with a small amount of C and O elements (Rasheed *et al.* 2024). Further, the EDS spectrum of CuO/Se revealed the presence of Cu, Se and O elements with a small amount of C element (Muthu and Sridharan 2018).

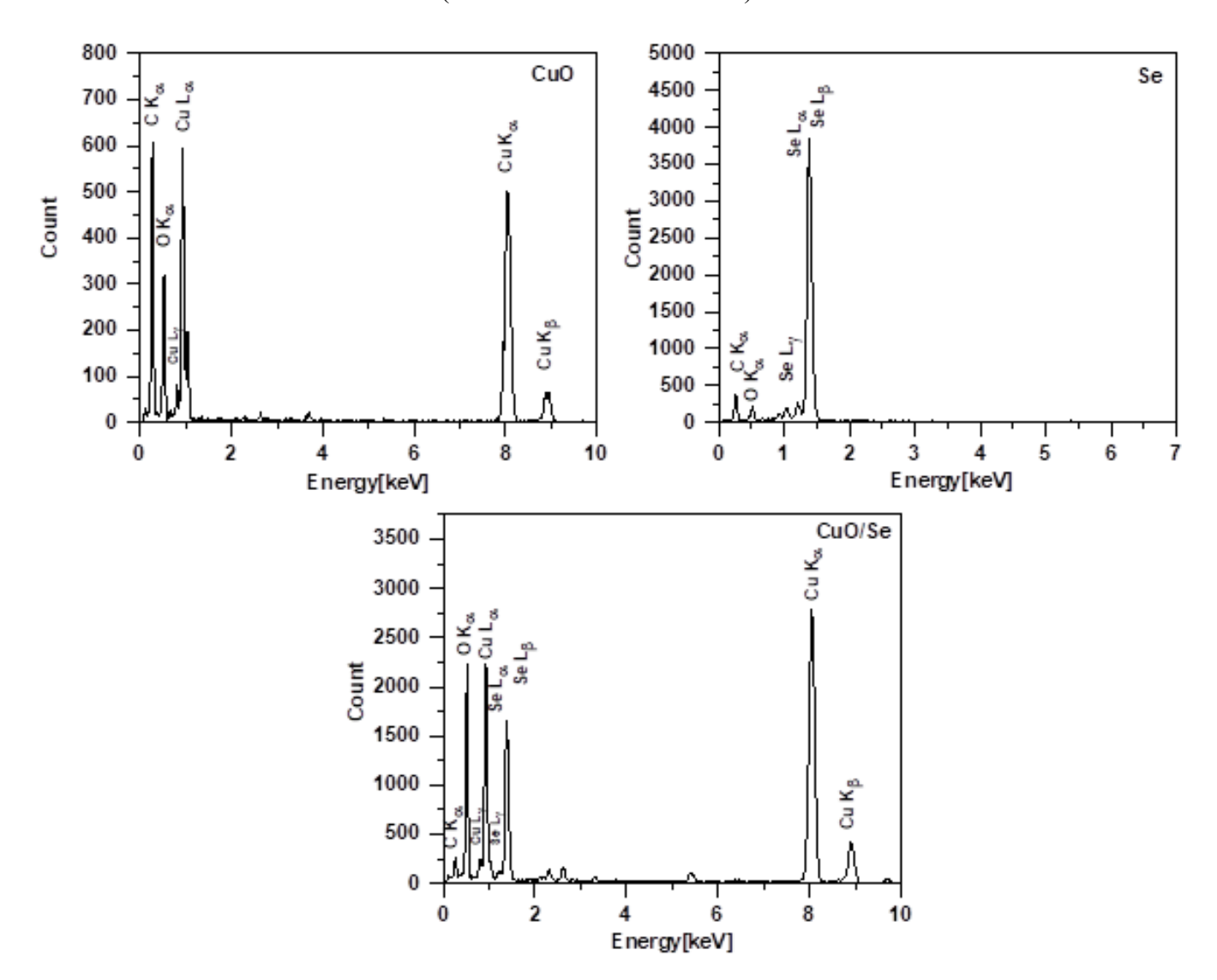


Fig. 4. shows the EDS spectra of the CuO, Se, and CuO/Se

The EDS elemental analysis of the CuO/Se showed that the atomic ratio of Cu/Se was almost 1:1. The presence of C and O elements in these NPs may be due to the hydroxyl and carboxyl groups that were found in phytochemical compounds of plant extract (Rong et al. 2012; Elkady et al. 2025). The presence of many phytochemicals of plant extract in CuO/Se leads to creating a protective shell around the particles, which has the potential to change of size and shape of particles (Elkady et al. 2025). Figure 5 displays the EDS

mapping images of CuO/Se. The EDS mapping analysis confirmed the presence of Cu (yellow), Se (red), and O (green) elements with a small amount of C (blue). Furthermore, all elements were uniformly distributed in this NPs

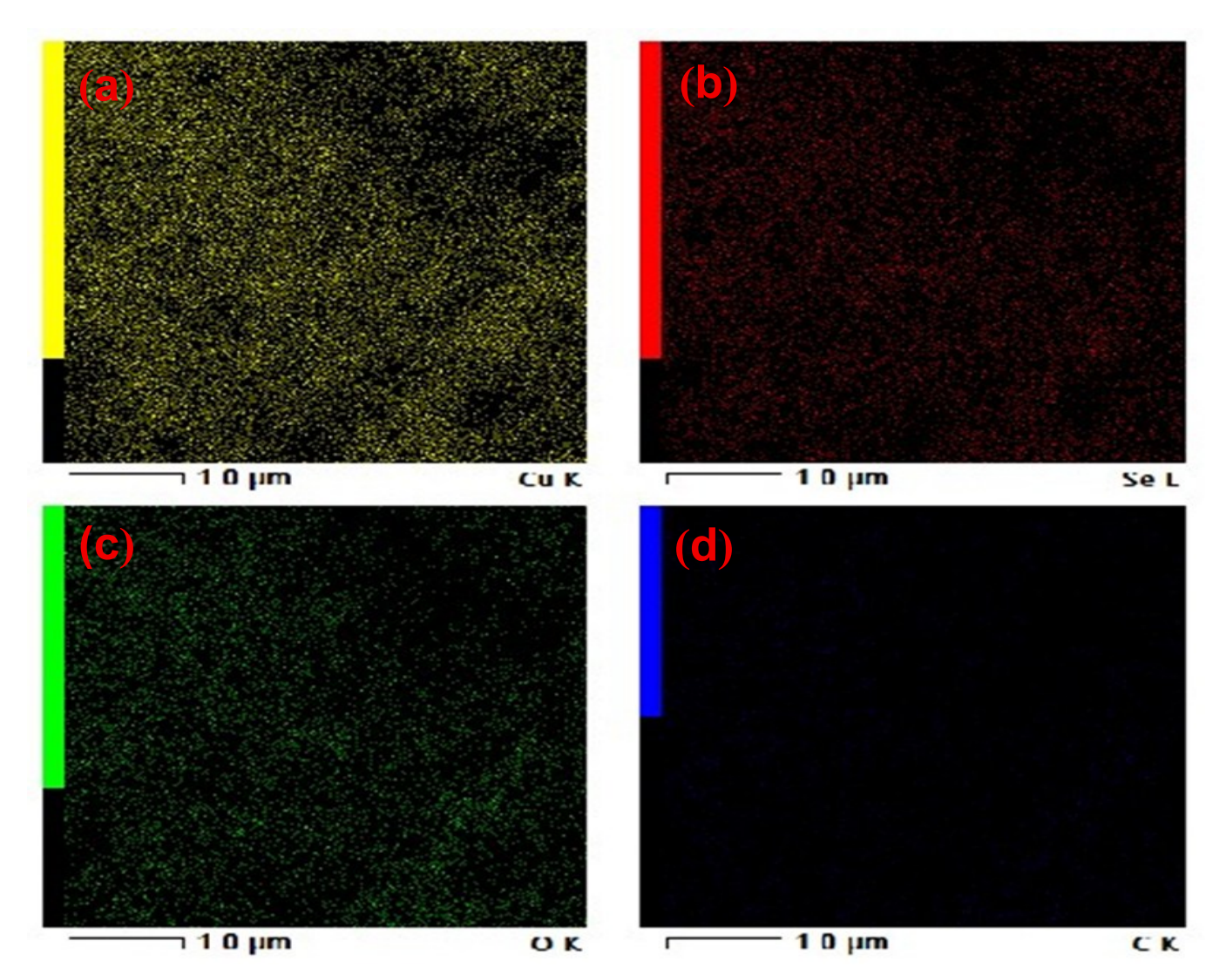


Fig. 5. EDS mapping of CuO/Se: (a) EDS mapping of Cu, (b): Se, (c): O, and (d): C atoms

Antimicrobial Activity

Table 1 provides data on the antimicrobial activity of *Anabasis setifera* extract, selenium nanoparticle, copper nanoparticle, and bimetallic biosynthesis CuO/Se agglomerates against various microbial strains, along with the performance of Ceftazidime / Clotrimazole as appositive control (Table 1 and Fig. 6).

When it is used only for bacterial infections, ceftazidime is a third-generation, broad-spectrum cephalosporin antibiotic that is effective against a variety of Gramnegative and certain Gram-positive bacteria. Conversely, clotrimazole is an antifungal medication that works best against fungi, such as *Candida albicans*.

The CuO/Se demonstrated the highest antimicrobial activity across all tested strains, with inhibition zones ranging from 19 mm (*Klebsiella pneumoniae*) to 26.1 mm (*Bacillus cereus*). Notably, CuO/Se agglomerates were effective against MRSA and *E. coli*,

strains that were resistant to individual SeNPs and CuNPs. This suggests a synergistic effect in the bimetallic system, enhancing antimicrobial potency and spectrum. The enhanced activity may stem from combined mechanisms, such as increased reactive oxygen species generation, membrane disruption, and metal ion release, which are more effective than monometallic nanoparticles alone (Abdelaziz *et al.* 2024).

Table 1. Antimicrobial Activity of *Anabasis setifera* Extract, Selenium Nanoparticle, Copper Nanoparticle, and Bimetallic Biosynthesis CuO/Se

| | Diameter of Inhibition Zone (mm) | | | | | |
|-------------------------------|----------------------------------|--------------------------------|------------------------------|-------------|----------------------------------|--|
| Microbial Strain | Anabasis setifera | Selenium Nano- particles | Cupper Nano- particles | CuO/Se] | Ceftazidime / Clotrimazole | |
| Klebsiella pneumonia | 0 | 13.5 ± 0.28 | 15.1 ± 0.44 | 19 ± 0.19 | 0 | |
| Staphylococcus aureus (MRSA) | 0 | 0 | 0 | 19.3 ± 0.33 | 0 | |
| Escherichia coli | 0 | 0 | 0 | 19.6 ± 0.88 | 0 | |
| Bacillus cereus | 0 | 0 | 14 ± 0.57 | 26.1 ± 0.72 | 0 | |
| Candida albicans ATCC10231 | 0 | 0 | 16.8 ± 0.44 | 21.6 ± 0.88 | 0 | |

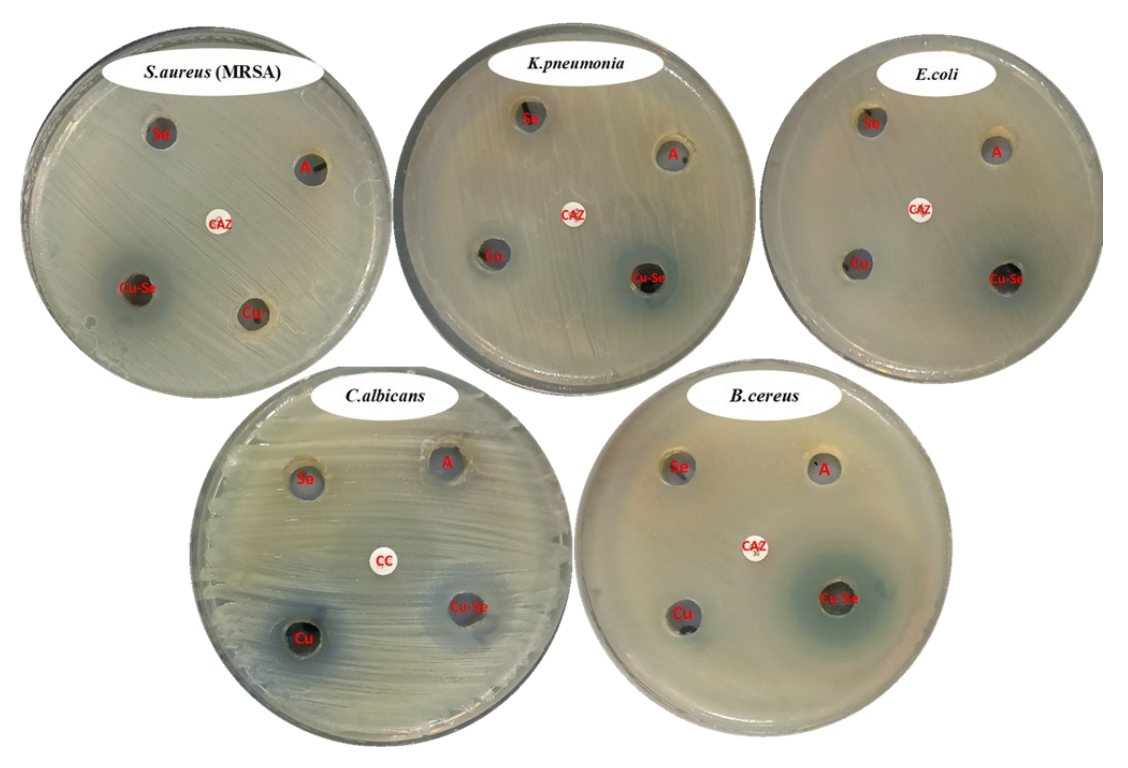


Fig. 6. Antimicrobial activity of (A = *Anabasis setifera* extract, Se = selenium NP, Cu= Copper NP, CAZ= Ceftazidime, CC= Clotrimazole, and Cu-Se= bimetallic biosynthesis CuO/Se

Determination of MIC of CuO/Se

Table 2 shows the MIC of CuO/Se against various bacterial strains and the fungus *Candida albicans*. The MIC values indicate the lowest concentration of the CuO/Se required to inhibit the growth of these microorganisms ranged between 62.5 to 125 μg/mL, as shown in Table 2 and Fig. 7. In this concept, Antony *et al.* (2022) found that, positively charged ions in the highest-performing Se-ZnO exhibit improved electrostatic interactions with negatively charged biological components, leading to the best MIC values based on the kind of microorganism. The interaction between the metal oxide and the biological components is thereby enhanced by its iconicity, leading to ideal MIC values.

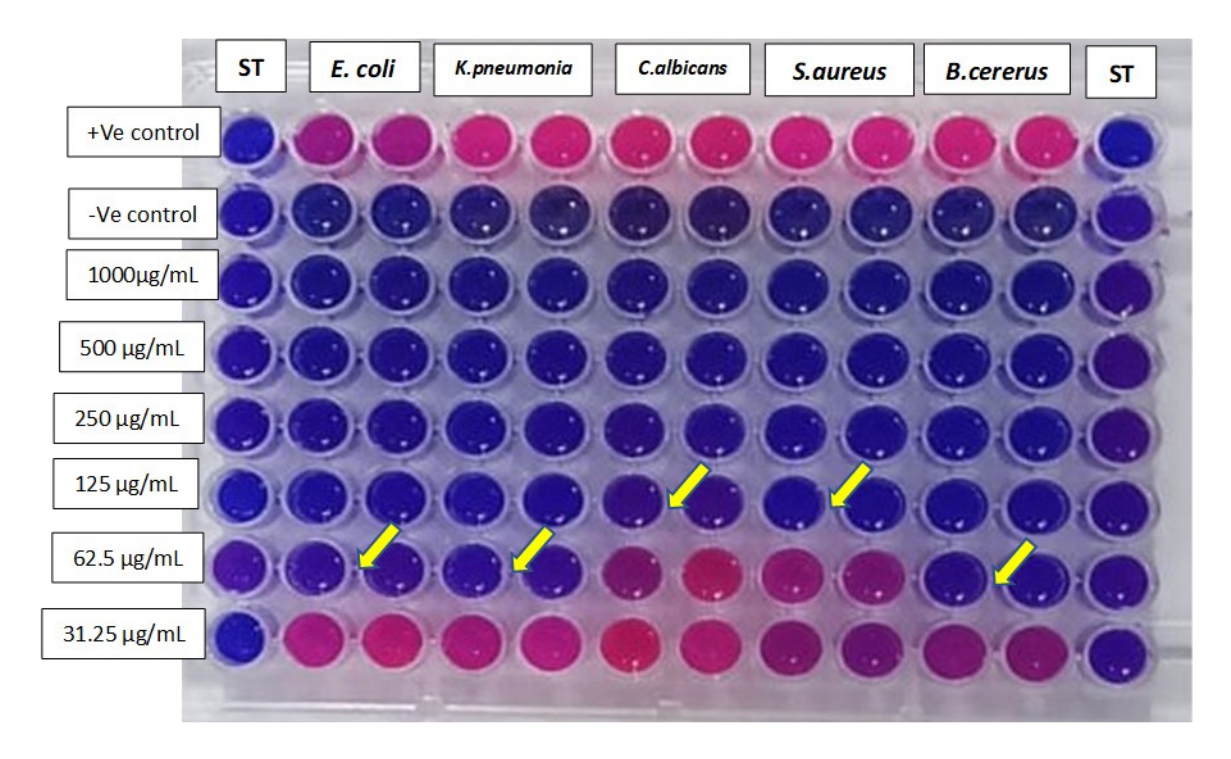


Fig. 7. CuO/Se MIC against *Candida albicans*, *Escherichia coli*, *Bacillus cereus*, *Klebsiella pneumoniae*, and *Staphylococcus aureus* (MRSA). Plates after 24 h in the Mueller Hinton (MH) broth resazurin assay (blue denotes growth inhibition, pink denotes growth). Compound-free Positive Control (MH broth + bacterial suspension + indicator); sterility control (MH broth + sterile distilled water + indicator) without bacteria is the Negative Control

Table 2. MIC of CuO/Se against Bacterial Strains and Candida albicans

| Microbial Strain | MIC of CuO/Se (μg/mL) | |
|------------------------------|-----------------------|--|
| Klebsiella pneumonia | 62.5 ± 0.76 | |
| Staphylococcus aureus (MRSA) | 125 ± 1.032 | |
| Escherichia coli | 62.5 ± 0.21 | |
| Bacillus cereus | 62.5 ± 1.05 | |
| Candida albicans | 125 ± 1.36 | |

Antioxidant Activity

Numerous studies have demonstrated that various natural and synthetic compounds exhibit significant antioxidant properties. In this study, the antioxidant activity was assessed using DPPH and ABTS methods, focusing on the DPPH radical-scavenging capacity (Fig. 8). Antioxidants are substances that neutralize reactive oxygen species (ROS), which are by-products generated during biological processes. These antioxidants are recognized as therapeutic agents due to their wide range of beneficial effects, including anti-atherosclerotic, anti-inflammatory, antiviral, antitumor, anticarcinogenic, antimutagenic, and antimicrobial activities (Lee *et al.* 2015; Kurutas 2015). In the current study, the antioxidant activity of CuO/Se at different concentrations (1000 to 7.81 μ g/mL) was measured using DPPH and ABTS methods, as shown in Fig. 7 Results showed that the antioxidant activity of CuO/Se with IC₅₀ = 150 μ g/mL compared to ascorbic acid (8.9 μ g/mL) for the DPPH method, while the IC₅₀ of CuO/Se for the ABTS method was 135 μ g/mL compared to ascorbic acid (7.61 μ g/mL).

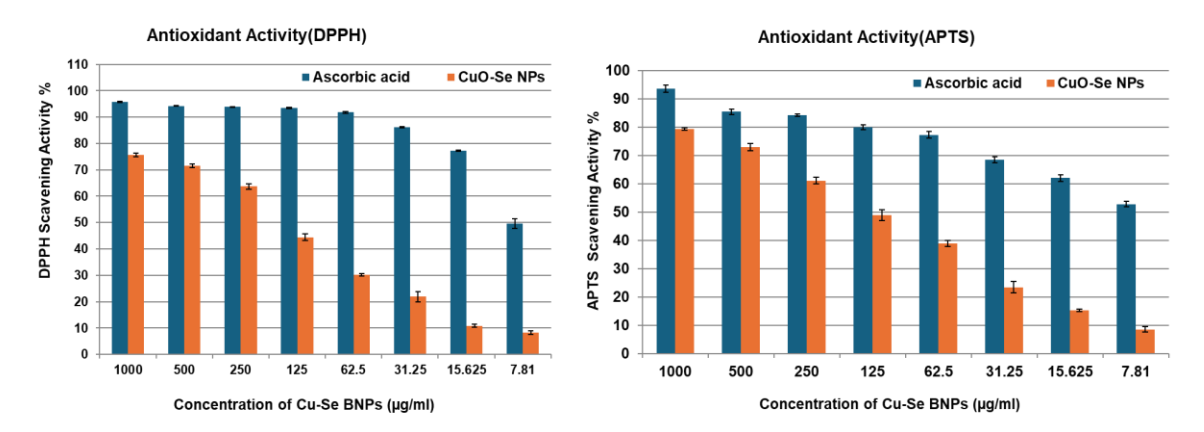


Fig. 8. Antioxidant activity of CuO/Se at different concentrations using DPPH and \overline{ABTS} methods

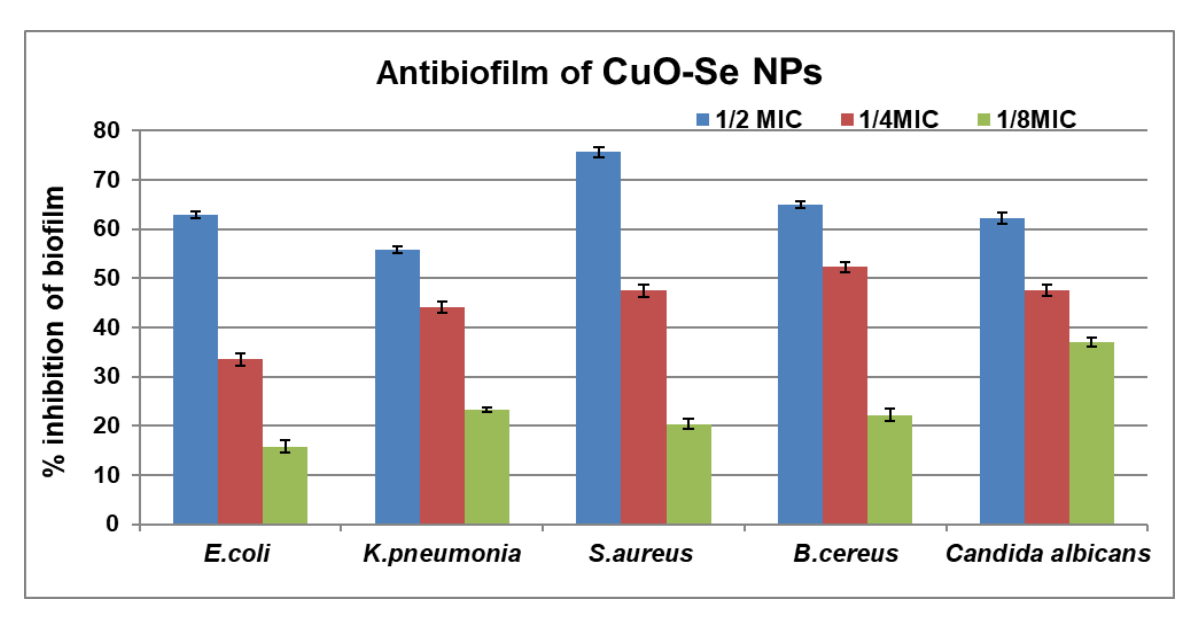


Fig. 9. Anti-biofilm activity of CuO/Se at different concentrations (1/2 MIC, 1/4 MIC, and 1/8 MIC)

Anti-Biofilm Ability

For all tested species, the results of the CuO/Se *in vitro* antibiofilm activity against tested pathogens (Fig. 9) showed that the CuO/Se decreased biofilm formation in a concentration-dependent manner. With *Staphylococcus aureus*, the greatest inhibition was observed at concentrations of 1/2 MIC and 1/8 MIC; the decrease ranged from 75.67 \pm 1.02% to 20.53 \pm 1.07%. Conversely, *Klebsiella pneumonia* showed the lowest reduction, with the percentage of inhibition varying between 55.765 \pm 0.756% and 23.27 \pm 0.48% at 1/2 MIC and 1/8 MIC doses, respectively.

Anticancer Activity of CuO/Se against Mcf7 and HepG2 cells

CuO/Se repressed the proliferation of Mcf7 and HepG2 cells, but CuO/Se showed more activity against HepG2 cells with IC50 322.5 μ g/mL (Table 3). The morphological changes were observed on the tested cancer cells depending on the level of inhibition (Figs. 10 and 11). The results demonstrated that, in comparison to the untreated cell lines, the tested concentrations of CuO/Se resulted in morphological changes in the cancerous cells, such as cell shrinkage, cell sheet destruction, irregular cell shape, and cytoplasmic condensation.

| | • | | |
|--------------------------|-----------|--------------|------|
| Concentration (µg/mL) | Toxic | HSD at 0.05 | |
| | Mcf7 | HepG2 | |
| Control | 0 | 0 | 000 |
| 31.25 | 0 | 0 | 0.01 |
| 62.5 | 0 | 0.28±0.01 | 0.36 |
| 125 | 0 | 1.65±0.04 | 0.68 |
| 250 | 0.14±0.01 | 48.87±0.65 | 5.65 |
| 500 | 0.36±0.02 | 79.51±1.89 | 2.78 |
| 1000 | 5.27±0.21 | 97.12±1.32 | 1.32 |
| IC ₅₀ (µg/mL) | - | 322.5 ± 1.74 | - |

Table 3. Anticancer Activity of CuO/Se

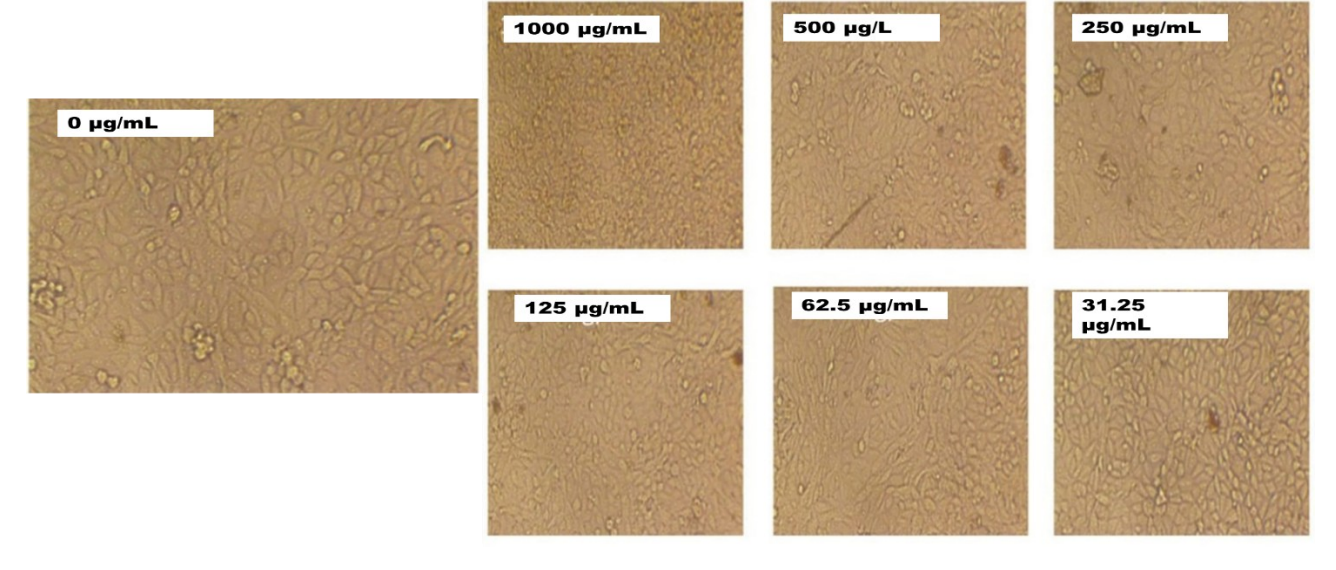


Fig. 10. Anticancer activity of CuO/Se against Mcf7 cells

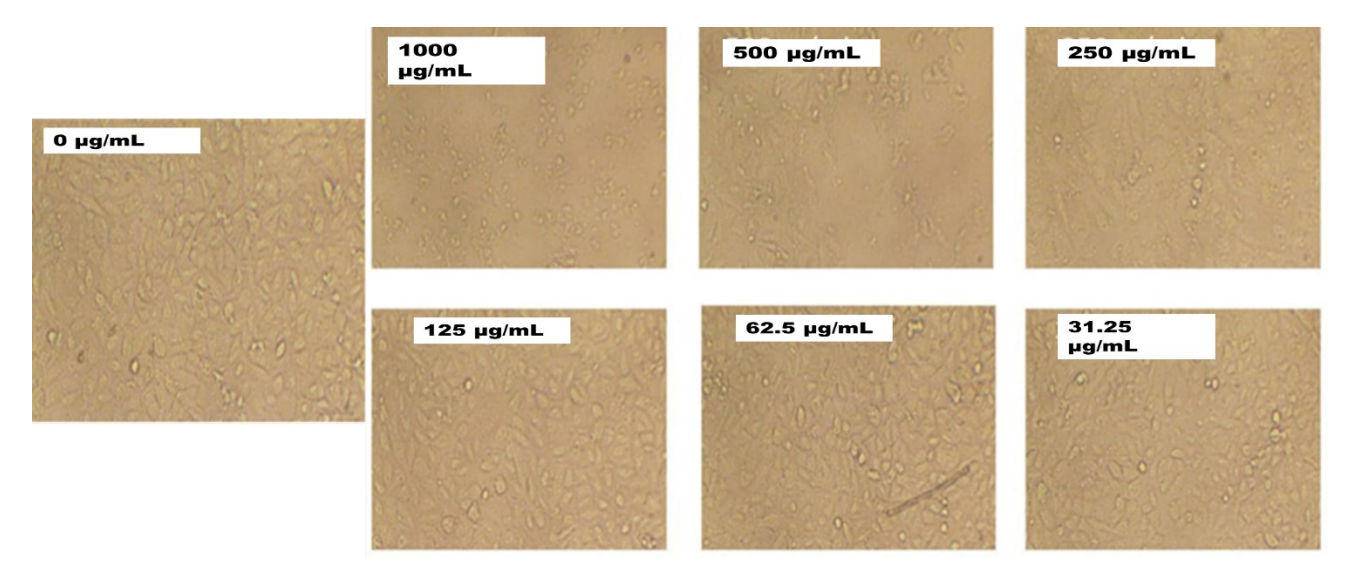


Fig. 11. Anticancer activity of CuO/Se against HepG2 cells

Recently, Se-CuO NPs showed improved anticancer activity against the breast cancer cell line MCF-7 (IC50 53.7 $\mu g/mL$) because of their electrical characteristics, which are derived from their frontier orbitals, electrostatic potentials, and their low hardness. It was also found that positive charges of NPs bind with the negative charges of biological molecules or the DNA bases bind.

The binding to the bases of DNA can be also provided by the solvated Cu ²⁺ ions that are released by the solvated Se-CuO particles to the cellular organelles. This occurs when electrons are transferred from the nitrogen lone pair of DNA bases to Cu²⁺. This then gives rise to the second competing mechanism for tumor cell mitosis, which mostly stops the process by damaging the nitrogenous bases of the DNA with the Cu²⁺ complex (Antony *et al.* 2022).

The quantities and physicochemical characteristics of the NPs, including their sizes, charges, and solubilities, make them prone to generate reactive oxygen species (ROS), which are deadly to tumor cells. The nanoparticles harm the cell membrane and cellular organelles, specifically the mitochondria and endoplasmic reticulum (ER), by triggering apoptosis through extrinsic and intrinsic cellular pathways, according to Chen *et al.* (2018). According to the findings of Saranya *et al.*'s (2023) study, the combination of Se NPs with apigenin increases the production of malondialdehyde in tumor cells, indicating that it may be used as a medication to treat breast cancer. Furthermore, with an IC50 of 18.9 µg mL, CuO NPs demonstrated decreased cell proliferation for MCF7. Additionally, increased production of lactate dehydrogenase (LDH), is most likely due to disruption to the cell membrane, resulting in leaks of cellular components, such as lactate dehydrogenase, through apoptosis (Mahmood *et al.* 2022).

CONCLUSIONS

An aqueous solution of *Anabasis setifera* shoot extract was used as a biological method for the first time to create both Se and CuO nanoparticles (NPs), as well as CuO/Se agglomerates of NPs. The antibacterial, antioxidant, antibiofilm, and anticancer activities of these NPs were assessed.

- 1. High resolution transmission electron microscopy (HR-TEM) confirmed the irregular, and spherical shapes of Cu and Se NPs, plus the CuO/Se agglomerates. The elemental dispersive X-ray spectroscopy (EDS) mapping of the CuO/Se NPs showed all elements were uniformly distributed in this sample.
- 2. The results showed that the antioxidant activity of CuO/Se agglomerates was 150 μg/mL for the DPPH radical method, compared to 8.9 μg/mL for ascorbic acid, and 135 μg/mL for the ABTS method for antioxidants activity, compared to 7.61 μg/mL for ascorbic acid.
- 3. These NPs also demonstrated the strongest antimicrobial action, with inhibition zones ranging from 19 mm for *Klebsiella pneumoniae* to 26.1 mm for *Bacillus cereus*. It is worth mentioning that CuO/Se agglomerates performed well against strains of *Staphylococcus aureus* (MRSA) and *Escherichia coli* that were resistant to both CuNPs and individual SeNPs.

ACKNOWLEDGMENTS

The authors extend their appreciation to the Deanship of Scientific Research at Northern Border University, Arar, KSA, for funding this research work through the project number "NBU-FFR-2025-337-04. The authors also extend their appreciation to Princess Nourah bint Abdulrahman University Researchers Supporting Project number (PNURSP2025R891), Princess Nourah bint Abdulrahman University, Riyadh, Saudi Arabia.

REFERENCES CITED

- Abdelaziz, A. M., Abdel-Maksoud, A. M., Fatima, S., Almutairi, S., Kiani, B. H., and Hashem, A. H. (2024). "Anabasis setifera leaf extract from arid habitat: A treasure trove of bioactive phytochemicals with potent antimicrobial, anticancer, and antioxidant properties," PLOS One 19(10), article e0310298. DOI: 10.1371/journal.pone.0310298
- Abd-ElGawad, A. M., Amin, M. A., Ismail, M. A., Ismail, M. K., Radwan, A. A., Sarker, T. C., El-Naggar, M. A., and Abdelkareem, E. M. (2025). "Selenium/copper oxide nanoparticles prepared with *Urtica urens* extract: Their antimicrobial, antioxidant, antihemolytic, anticoagulant, and plant growth effects," *BioResources* 20(2), 2791-2810. DOI: 10.15376/biores.20.2.2791-2810
- Al-Rajhi, A. M. H., Yahya, R., Bakri, M. M. Y. R., and Abdelghany, T. M. (2022). "In situ green synthesis of Cu-doped ZnO based polymers nanocomposite with studying antimicrobial, antioxidant and anti-inflammatory activities," Appl. Biol. Chem. 65,

- article 35. DOI: 10.1186/s13765-022-00702-0
- Amin, M. A., Shahhat, I. M., Ismail, M. A., Nowwar, A. I., Elsheikh, S. Y. S., El-khawaga, H. A., Abdelwahab, A. T., Abdelfattah, M. A., Elsherbeny, S. A., Abdel-Mageed, A. M., Abdein, M. A., and Bedawy, I. (2024). "Vicia faba overcomes drought stress by spraying with xerophytic Anabasis setifera extract," Edelweiss Applied Science and Technology 8(6), 8008-8022. DOI: 10.55214/25768484.v8i6.3737
- Amin, M. A. A., Abu-Elsaoud, A. M., Nowwar, A. I., Abdelwahab, A. T., Awad, M. A., Hassan, S. E. D., and Elkelish, A. (2024). "Green synthesis of magnesium oxide nanoparticles using endophytic fungal strain to improve the growth, metabolic activities, yield traits, and phenolic compounds content of *Nigella sativa L.*," *Green Processing and Synthesis* 13(1), article 20230215. DOI: 10.1515/gps-2023-0215
- Amin, M. A., Algamdi, N. A., Waznah, M. S., Bukhari, D. A., Alsharif, S. M., Alkhayri, F., Abdel-Nasser, M., Fouda, A. (2025). "An insight into antimicrobial, antioxidant, anticancer, and antidiabetic activities of trimetallic Se/ZnO/CuO nanoalloys fabricated by aqueous extract of *Nitraria retusa*," *Journal of Cluster Science* 36(1), 1-15. DOI: 10.1007/s10876-024-02742-6
- Antony, D., Balasubramanian, K., and Yadav, R. (2022). "Experimental and computational studies of phytomediated selenium-CuO and ZnO nanoparticlespotential drugs for breast cancer," *Journal of Molecular Structure* 1263, article ID 133113. DOI: 10.1016/j.molstruc.2022.133113
- Asaad, A. M., Saied, S. A., Torayah, M. M., Abu-Elsaad, N., and Awad, S. M. (2025). "Antibacterial activity of selenium nanoparticles/copper oxide (SeNPs/CuO) nanocomposite against some multi-drug resistant clinical pathogens," *BMC Microbiology* 25(1), article ID 33. DOI:10.1186/s12866-025-03743-9
- Chen, L., Wu, L. Y., and Yang, W. X. (2018). "Nanoparticles induce apoptosis *via* mediating diverse cellular pathways," *Nanomedicine* 13(22), 2939-2955. DOI: 10.2217/nnm-2018-0167
- Duman, F., Ocsoy, I., and Kup, F. O. (2016). "Chamomile flower extract-directed CuO nanoparticle formation for its antioxidant and DNA cleavage properties," *Materials Science and Engineering:* C 60, 333-338. DOI:10.1016/j.msec.2015.11.052
- El-Batal, A. I., Ismail, M. A., Amin, M. A., El-Sayyad, G. S., and Osman, M. S. (2023). "Selenium nanoparticles induce growth and physiological tolerance of wastewater-stressed carrot plants," *Biologia* 78(9), 2339-2355. DOI: 10.1007/s11756-023-01401-x
- El-Didamony, S. E., Kalaba, M. H., Sharaf, M. H., El-Fakharany, E. M., Osman, A., Sitohy, M., and Sitohy, B. (2024). "Melittin alcalase-hydrolysate: A novel chemically characterized multifunctional bioagent; antibacterial, anti-biofilm and anticancer," *Frontiers in Microbiology* 15, article 1419917. DOI: 10.3389/fmicb.2024.1419917
- Elkady, F. M., Badr, B. M., Saied, E., Hashem, A. H., Abdel-Maksoud, M. A., Fatima, S., Malik, A., Aufy, M., Hussein, A. M., Abdulrahman, M. S., *et al.* (2025). "Green biosynthesis of bimetallic copper oxide-selenium nanoparticles using leaf extract of *Lagenaria siceraria*: Antibacterial, anti-virulence activities against multidrugresistant *Pseudomonas aeruginosa*," *International Journal of Nanomedicine* 2025(20), 4705-4727. DOI: 10.2147/IJN.S497494
- El-Sayed, M. H., Alshammari, F. A., and Sharaf, M. H. (2022). "Antagonistic potentiality of actinomycete-derived extract with anti-biofilm, antioxidant, and cytotoxic capabilities as a natural combating strategy for multidrug-resistant ESKAPE

- pathogens," *Journal of Microbiology and Biotechnology* 33(1), article 61. DOI: 10.4014/jmb.2211.11026
- El-Sherbiny, G. M., Kalaba, M. H., Sharaf, M. H., Moghannem, S. A., Radwan, A. A., Askar, A. A., Ismail, M. K. A., El-Hawary, A. S., and Abushiba, M. A. (2022). "Biogenic synthesis of CuO-NPs as nanotherapeutic approaches to overcome multidrug-resistant *Staphylococcus aureus* (MDRSA)," *Artificial Cells, Nanomedicine, and Biotechnology* 50(1), 260-274. DOI: 10.1080/21691401.2022.2126492
- Gad, E. S., Salem, S. S., Selim, S., Almuhayawi, M. S., Alruhaili, M. H., Al Jaouni, S. K., and Owda, M. E. (2025). "A comprehensive study on characterization of biosynthesized copper-oxide nanoparticles, their capabilities as anticancer and antibacterial agents, and predicting optimal docking poses into the cavity of *S. aureus* DHFR," *PLOS One* 20(4), article e0319791. DOI: 10.1371/journal.pone.0319791
- Hong, Z.-S., Cao, Y., and Deng, J.-F. (2002). "A convenient alcohothermal approach for low temperature synthesis of CuO nanoparticles," *Materials Letters* 52(1-2), 34-38. DOI: 10.1016/S0167-577X(01)00361-5
- Hsueh, P.-R., Ko, W.-C., Wu, J.-J., Lu, J.-J., Wang, F.-D., Wu, H.-Y., Wu. T., Teng, L.-J. (2010). "Consensus statement on the adherence to Clinical and Laboratory Standards Institute (CLSI) Antimicrobial Susceptibility Testing Guidelines (CLSI-2010 and CLSI-2010-update) for Enterobacteriaceae in clinical microbiology laboratories in Taiwan," *Journal of Microbiology, Immunology and Infection* 43(5), 452-455.
- Khowdiary, M. M., Alatawi, Z., Alhowiti, A., Amin, M. A., Daghistani, H., Albaqami, F. M. K., Abdel-Rahman, M. A. Ghareeb, A., Shaer, N. A., Shawky, A. M., et al. (2024). "Phytochemical analysis and multifaceted biomedical activities of Nitraria retusa extract as natural product-based therapies," Life 14(12), article 1629. DOI: 10.3390/life14121629
- Kurutas, E. B. (2015). "The importance of antioxidants which play the role in cellular response against oxidative/nitrosative stress: Current state," *Nutrition Journal* 15, 1-22. DOI: 10.1186/s12937-016-0186-5
- Lee, K. J., Oh, Y. C., Cho, W. K., and Ma, J. Y. (2015). "Antioxidant and anti-inflammatory activity determination of one hundred kinds of pure chemical compounds using offline and online screening HPLC assay," *Evidence-Based Complementary and Alternative Medicine* 2015(1), article 165457. DOI: 10.1155/2015/165457
- Mahmood, R. I., Kadhim, A. A., Ibraheem, S., Albukhaty, S., Mohammed-Salih, H. S., Abbas, R. H., Jabir, M. S., Mohammed, M. K. A., Nayef, U. M., AlMalki, F. A., *et al.* (2022). "Biosynthesis of copper oxide nanoparticles mediated *Annona muricata* as cytotoxic and apoptosis inducer factor in breast cancer cell lines," *Scientific Reports* 12(1), article 16165. DOI: 10.1038/s41598-022-20360-y
- Muthu, S., and Sridharan, M. B. (2018). "Synthesis and characterization of two dimensional copper selenide (CuSe) nanosheets," *Materials Today: Proceedings* 5(11), 23161-23168. DOI: 10.1016/j.jece.2024.113125
- Nowrouzi, I., Mohammadi, A. H., and Khaksar Manshad, A. (2025). "A non-ionic green surfactant extracted from the Anabasis setifera plant for improving bulk properties of CO2-foam in the process of enhanced oil recovery from carbonate reservoirs," *The Canadian Journal of Chemical Engineering* 103(2), 590-605. DOI: 10.1002/cjce.25401

- Rasheed, R., Bhat, A., Singh, B., and Tian, F. (2024). "Biogenic synthesis of selenium and copper oxide nanoparticles and inhibitory effect against multi-drug resistant biofilm-forming bacterial pathogens," *Biomedicines* 12(5), article 994. DOI: 10.3390/biomedicines12050994
- Rong, F., Bai, Y., Chen, T., and Zheng, W. (2012). "Chemical synthesis of Cu₂Se nanoparticles at room temperature," *Materials Research Bulletin* 47(1), 92-95. DOI: 10.1021/jp051328n
- Ryntathiang, I., Jothinathan, M. K. D., Behera, A., Saravanan, S., and Murugan, R. (2024). "Comparative bioactivity analysis of green-synthesized metal (cobalt, copper, and selenium) nanoparticles," *Cureus* 16(3), article ID 55933. DOI: 10.7759/cureus.55933
- Sahooli, M., Sabbaghi, S., and Saboori, R. (2012). "Synthesis and characterization of mono sized CuO nanoparticles," *Materials Letters* 81, 169-172. DOI: 10.1016/j.matlet.2012.04.148
- Saranya, T., Ramya, S., Kavithaa, K., Paulpandi, M., Cheon, Y.-P., Harysh Winster, S., and Narayanasamy, A. (2023). "Green synthesis of selenium nanoparticles using solanum nigrum fruit extract and its anti-cancer efficacy against triple negative breast cancer," *Journal of Cluster Science* 34(4), 1709-1719. DOI: 10.1007/s10876-022-02334-2
- Selim, S., Almuhayawi, M. S., Alruhaili, M. H., Tarabulsi, M. K., Saddiq, A. A., Elamir, M. Y. M., and Al Jaouni, S. K. (2025a). "Pharmacological applications and plant stimulation under sea water stress of biosynthesis bimetallic ZnO/MgO NPs," *Scientific Reports* 15(1). DOI: 10.1038/s41598-025-87881-0
- Selim, S., Saddiq, A. A., Ashy, R. A., Baghdadi, A. M., Alzahrani, A. J., Mostafa, E. M., Al Jaouni, S. K., Elamir, M. Y. M., Amin, M. A., Salah, A. M., *et al.* (2025b). "Bimetallic selenium/zinc oxide nanoparticles: Biological activity and plant biostimulant properties," *AMB Express* 15(1), 1-11. DOI: 10.1186/s13568-024-01808-y
- Sharaf, M. H. (2020). "Evaluation of the antivirulence activity of ethyl acetate extract of *Deverra tortuosa* (Desf) against *Candida albicans*," *Egyptian Pharmaceutical Journal* 19(2), article 188. DOI: 10.4103/epj.epj-10-20
- Sharaf, M. H., El-Sherbiny, G. M., Moghannem, S. A., Abdelmonem, M., Elsehemy, I. A., Metwaly, A. M., and Kalaba, M. H. (2021). "New combination approaches to combat methicillin-resistant *Staphylococcus aureus* (MRSA)," *Scientific Reports* 11(1), article 4240. DOI: 10.1038/s41598-021-82550-4
- Soliman, M. K., Amin, M. A.-A., Nowwar, A. I., Hendy, M. H., and Salem, S. S. (2024). "Green synthesis of selenium nanoparticles from *Cassia javanica* flowers extract and their medical and agricultural applications," *Scientific Reports* 14(1), article 26775. DOI: 10.1038/s41598-024-77353-2
- Thirupathi, B., Pongen, Y. L., Kaveriyappan, G. R., Dara, P. K., Rathinasamy, S., Vinayagam, S., Sundaram I. T., Hyun, B. K., Durairaj, T., and Sekar, S. K. R. (2024). "Padina boergesenii mediated synthesis of Se-ZnO bimetallic nanoparticles for effective anticancer activity," Frontiers in Microbiology 15, article 1358467. DOI: 10.3389/fmicb.2024.1358467
- Tugarova, A. V., Mamchenkova, P. V., Dyatlova, Y. A., and Kamnev, A. A. (2018). "FTIR and Raman spectroscopic studies of selenium nanoparticles synthesised by the

- bacterium Azospirillum thiophilum," Spectrochimica Acta Part A: Molecular and Biomolecular Spectroscopy 192, 458-463.
- Van de Loosdrecht, A., Beelen, R., Ossenkoppele, G., Broekhoven, M., and Langenhuijsen, M. (1994). "A tetrazolium-based colorimetric MTT assay to quantitate human monocyte mediated cytotoxicity against leukemic cells from cell lines and patients with acute myeloid leukemia," *Journal of Immunological Methods* 174(1-2), 311-320. DOI: 10.1016/0022-1759(94)90034-5
- Vinu, D., Govindaraju, K., Vasantharaja, R., Amreen Nisa, S., Kannan, M., and Vijai Anand, K. (2021). "Biogenic zinc oxide, copper oxide and selenium nanoparticles: Preparation, characterization and their anti-bacterial activity against *Vibrio parahaemolyticus*," *Journal of Nanostructure in Chemistry* 11, 271-286. DOI: 10.1007/s40097-020-00365-7

Article submitted: July 17, 2025; Peer review completed: August 23, 2025; Revised version received September 9, 2025; Accepted: September 10, 2025; Published: October 3, 2025.

DOI: 10.15376/biores.20.4.10008-10027